Springer

KSME

Journal of Mechanical Science and Technology 31 (5) (2017) 2143~2154
www.springerlink.com/content/1738-494x(Print)/1976-3824(Online)
DOI 10.1007/s12206-017-0410-z

Effects of different coupling models of a helical gear system on vibration characteristics †

Qibin Wang[1], Zhanwei Li[2], Hui Ma[2,3,*] and Bangchun Wen[2]

[1]*School of Mechano-Electronic Engineering, Xidian University, Xi'an 710071, China*
[2]*School of Mechanical Engineering and Automation, Northeastern University, Shenyang 110819, China*
[3]*State Key Laboratory for Strength and Vibration of Mechanical Structures, Xi'an Jiaotong University, Xi'an 710049, China*

(Manuscript Received July 21, 2016; Revised November 25, 2016; Accepted January 8, 2017)

Abstract

Time-varying mesh stiffness (TVMS) and the dynamic coupling between the helical gears have a great influence on the vibration characteristics of a helical gear rotor system. Considering the effects of TVMS and adopting two coupling models (lateral-torsional coupling model and lateral-torsional-axial-swing coupling model), the dynamic behavior of a helical gear system was studied. First, an analytical model was used to analyze TVMS of a helical gear pair where the helical tooth is simulated by many spur tooth slices along the direction of the tooth width and the mesh stiffness of each slice is calculated using the energy method. Then, considering the effects of the TVMS excitation, the finite element model of a helical gear rotor system was established. Gear mesh was simulated by the above-mentioned two coupling models to investigate the effects of coupling forms on the system vibration characteristics. The strain energy was used to distinguish the dominant mode and dominant shaft of a gear system in natural characteristics analysis. The results show that the full coupling model can analyze accurately the vibration characteristics of the system and the axial and swing motions cannot be ignored in vibration analysis. Finally, the effects of helix angle on TVMS and vibration responses of a helical gear system were also studied.

Keywords: Helical gear; Time-varying mesh stiffness; Natural characteristics; Vibration response; Strain energy

1. Introduction

Helical gear pairs are widely used to transmit power and motion; their mechanical behavior and working performance have a great influence on the whole machine. Some factors, such as Time-varying mesh stiffness (TVMS) and lateral-torsional coupled vibration, will affect the vibration characteristics of gear systems. At present, there are many studies on these two aspects. Many works for calculating TVMS and Loaded transmission error (LTE) have been performed [1-4]. Wan et al. [1] obtained the TVMS of a helical gear pair by potential energy method, and verified the simulated results by comparing the results obtained from the Finite element (FE) method and ISO standard. By simplifying the helical gear as many spur gear slices along the gear width direction, Wang and Zhang [2] developed a model for calculating TVMS and stress of a helical gear pair. Gu et al. [3] presented some analytical formulae for TVMS calculation of solid spurs and helical gears. Hedlund and Lehtovaara [4] presented a method to calculate TVMS of helical gear pairs. In their model, the combined stiffness for tooth and foundation is determined using linear FE approach, and the contact stiffness is obtained by Hertzian contact formulas.

Besides the time-varying mesh characteristics due to tooth engagement, the vibration behaviors caused by TVMS and the vibration coupling of helical gear pairs have also been widely considered [5-15]. Kahraman [5] presented a mathematical model of a helical gear system with an invariable mesh stiffness, which considers the coupling of lateral, torsional, axial and swing motions caused by gear engagement. For the coupling effects of transverse, torsional and axial vibrations due to gear meshing, Choi et al. [6] investigated the vibration responses of a geared rotor system in a 28-MW turbo set. Kubur et al. [7, 8] presented a dynamic model for simulating the dynamic behavior of a helical gear rotor system with multiple shafts. In their model, the shafts are modeled using FE method and the helical gear pairs are modeled using a lumped mass model. Based on Kubur's model, Zhang et al. [9] proposed a general FE model of helical gear systems. Their model accounts for the effects of geometric eccentricity, gear meshing, bearing flexibility, and shaft flexibility. Kang and Kahraman [10] proposed a mathematical model of a double-helical gear system in which the time-invariant mesh stiffness of gear pairs is considered, and analyzed the vibration characteristics of the system by the theoretical simulation and experiment. Kang

*Corresponding author. Tel.: +86 24 83684491, Fax.: +86 24 83684491
E-mail address: mahui_2007@163.com
† Recommended by Associate Editor Eung-Soo Shin

and Kahraman [11] proposed an improved method for measuring the acceleration responses of geared rotor systems in lateral, torsional and axial directions. Velex et al. [12] developed a dynamic model of gear rotor systems in which the gear pair is simulated using a lumped-parameter method and the shafts are simulated using two-node shaft elements with concentrated stiffness and mass elements. Nishino [13] analyzed the dynamic responses of a helical geared system under three types of excitation using an integrated excitation model. In his model, the gear tooth engagement and moving load are simulated by the multiple springs and mesh excitation forces, respectively. Eritenel and Park [14] simulated gear engagement using multiple parallel stiffness along the contact lines, and studied the nonlinear vibrations of gear pairs considering the effects of partial contact loss. Chen et al. [15] analyzed the vibration characteristics of a double-helical geared rotor system where the shafts are modeled using Timoshenko beams, and the gears are simulated using rigid lumped masses. Abbes et al. [16] presented a sub-structure model of a gearbox where the shafts connected with a gear pair are considered as one sub-structure and the housing is regarded as another sub-structure, and analyzed the effects of Transmission error (TE) on the vibration behavior of the gearbox system. On the basis of the dynamic contact theory, Wu et al. [17] studied the dynamic responses of a helical gear system considering the effects of tooth profile modification, and the simulation results are also verified by experimental results.

The above literature analysis shows that the time-invariant mesh stiffness is mostly used to analyze the linear vibration responses of the helical gear systems [5-10, 15], or some simplified TVMS such as a rectangular waveform is used [16]. To accurately predict the dynamic responses of helical gear systems, an accurate dynamic model connecting the gear parameters such as helix angle and normal module with the system vibration is essential. This model can accurately quantify the effects of helix angle on the TVMS and mesh stiffness matrix due to the lateral-torsional-axial-swing coupling vibration. In this study, we propose an accurate dynamic modeling for a helical gear rotor system with TVMS based on our previous work [9]. Moreover, the effects of lateral-torsional coupling and lateral-torsional-axial-swing coupling on natural frequencies are also quantified using modal strain energy, and their effects on the system dynamic responses are also evaluated. Finally, the effects of helix angle on TVMS and vibration responses of a helical gear system are also discussed.

2. TVMS calculation of a helical gear pair

Contact lines of a helical gear are diagonal of the gear axes (see Fig. 1). So the stiffness of a helical tooth is changing along the contact lines. In addition, the length of the contact lines will vary with the changing mesh positions. Therefore, it is more difficult to calculate the mesh stiffness of helical gear pairs than that of spur gear pairs.

Based on sliced tooth theory, the helical gear pair is simulated by many spur gear slices along the gear width direction. For the spur gear slice, the face-width is relatively small. Based on our earlier work [2], mesh stiffness and load sharing factor can be expressed as:

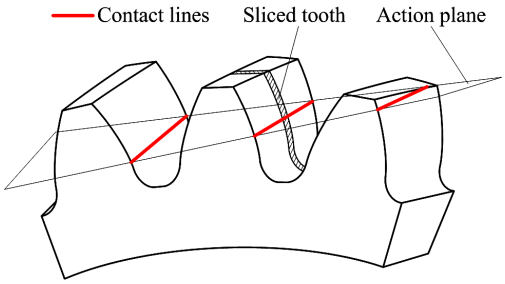

Fig. 1. Schematic of a three-dimensional helical gear.

$$K = \sum_{i=1}^{N} k_i \ , \quad Lsf_i = \frac{k_i}{K}, \tag{1}$$

where N represents the number of sliced tooth pairs under engagement. k_i is the mesh stiffness of the ith sliced tooth pair. To obtain the mesh stiffness and load sharing factor, it is necessary to identify which sliced tooth pairs are in mesh and the mesh stiffness of each sliced tooth pair k_i.

2.1 Determination of the sliced tooth pairs in mesh

The instantaneous pressure angle of each sliced tooth in mesh varies with the gear rotation. The instantaneous pressure angle of the sliced tooth i can be written as:

$$\tau_i = \arctan(\varphi_{1,n} + \varphi_{2,n}) , \tag{2}$$

where $\varphi_{1,n}$ and $\varphi_{2,n}$ (n = 1, 2 represent the pinion and gear, respectively) of the sliced tooth i can be written as:

$$\begin{cases} \varphi_{1,1} = \varphi_0 + (k-1)\dfrac{\pi}{2z_1} + b_i \cdot \tan\beta_b / r_{b1} - \varphi_{2,1} \\ \varphi_{1,2} = \dfrac{a \cdot \sin\varphi_{12} - r_{b1} \cdot (\varphi_{1,1} + \varphi_{2,1})}{r_{b2}} - \varphi_{2,2} \end{cases}, \tag{3}$$

$$\begin{cases} \varphi_{2,1} = \dfrac{\pi}{2z_1} + \mathrm{inv}\varphi_{12} \\ \varphi_{2,2} = \dfrac{\pi}{2z_2} + \mathrm{inv}\varphi_{12} \end{cases}, \tag{4}$$

where z_1 and z_2 denote the tooth numbers of the pinion and gear. Detailed parameters can be found in Ref. [2].

If a sliced tooth pair is in mesh, the instantaneous pressure angle must be greater than the minimum pressure angle τ_b and less than the maximum pressure angle τ_e (see Fig. 2). τ_b and τ_e can be calculated as:

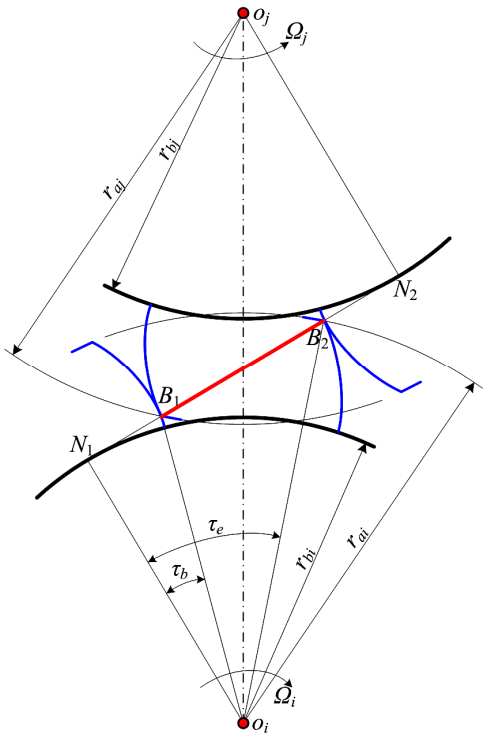

Fig. 2. Engagement schematic of a gear pair.

$$\begin{cases} \tau_b = \arctan\left(\dfrac{N_1B_1}{r_{bi}}\right) \\ \tau_e = \arctan\left(\dfrac{N_1B_1 + B_1B_2}{r_{bi}}\right) \end{cases}. \tag{5}$$

2.2 Mesh stiffness of a sliced tooth pair

In this section, a spur gear pair is used to replace the sliced tooth pair. So the sliced tooth is considered as a non-uniform cantilever beam as shown in Fig. 3 and mesh stiffness of a sliced tooth pair can be calculated by the potential energy method. The total energy stored in the gear pair includes bending energy, shear energy, axial compressive energy, gear foundation energy and Hertzian contact energy. So the mesh stiffness of a sliced tooth pair can be expressed as [2, 19, 20]:

$$k_i = \frac{1}{\dfrac{1}{k_h}+\dfrac{1}{k_{b1}}+\dfrac{1}{k_{s1}}+\dfrac{1}{k_{a1}}+\dfrac{1}{k_{f1}}+\dfrac{1}{k_{b2}}+\dfrac{1}{k_{s2}}+\dfrac{1}{k_{a2}}+\dfrac{1}{k_{f2}}}, \tag{6}$$

where k_b, k_s, k_a, k_f and k_h denote bending stiffness, shear stiffness, axial compressive stiffness, gear foundation stiffness and Hertzian contact stiffness, respectively. Subscripts 1 and 2 represent the pinion and the gear, respectively. Bending stiffness, shear stiffness, axial compressive stiffness, gear foundation stiffness and Hertzian contact stiffness can be calculated

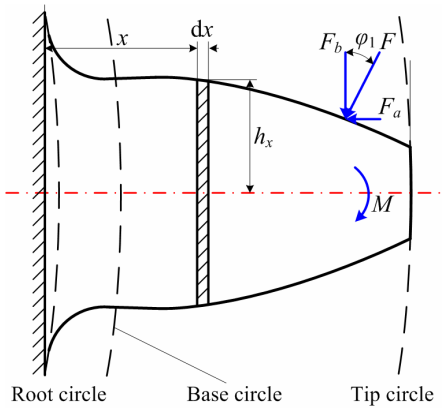

Fig. 3. Cantilever beam model of a tooth.

as [2]:

$$\frac{1}{k_b} = \int_{-\varphi_1}^{\varphi_2} \frac{3[1+(\varphi_2-\varphi)\sin\varphi\cos\varphi_1-\cos\varphi\cos\varphi_1]^2}{2E\Delta l[(\varphi_2-\varphi)\cos\varphi+\sin\varphi]^3}(\varphi_2-\varphi)\cos\varphi\,\mathrm{d}\varphi, \tag{7}$$

$$\frac{1}{k_s} = \int_{-\varphi_1}^{\varphi_2} \frac{1.2(1+\nu)(\varphi_2-\varphi)\cos\varphi\cos^2\varphi_1}{E\Delta l[(\varphi_2-\varphi)\cos\varphi+\sin\varphi]}\mathrm{d}\varphi, \tag{8}$$

$$\frac{1}{k_a} = \int_{-\varphi_1}^{\varphi_2} \frac{(\varphi_2-\varphi)\cos\varphi\sin^2\varphi_1}{2E\Delta l[(\varphi_2-\varphi)\cos\varphi+\sin\varphi]}\mathrm{d}\varphi, \tag{9}$$

$$\frac{1}{k_f} = \frac{\cos^2\varphi_1}{E\Delta l}\left\{L^*\left(\frac{u_f}{S_f}\right)^2 + M^*\left(\frac{u_f}{S_f}\right) + P^*(1+Q^*\tan^2\varphi_1)\right\}, \tag{10}$$

$$k_h = \frac{\pi E\Delta l}{4(1\text{-}\mu^2)}, \tag{11}$$

where Δl is the width of the sliced tooth pair and other parameters are given in Ref. [2].

Two helical gear pairs with different helix angles are used to calculate TVMS, where the gear pair 1 consists of gears 1 and 2, and the gear pair 2 consists of gears 3 and 4. These gear parameters are listed as follows: the tooth numbers of gears 1, 2, 3 and 4 are 52, 72, 22 and 79, respectively. The gear widths of four gears are all 20 mm. TVMS of the helical gear pairs 1 and 2 under different helix angles β_{ij} = 0°, 5°, 10°, 15°, 20° are shown in Fig. 4. For the gear pair 1, the fluctuation of TVMS decreases with the increasing helix angle except for β_{ij} = 15°, as shown in Fig. 4(a). This is because of the fluctuation value of mesh stiffness decreases when the transverse contact ratio or the face contact ratio is close to an integer. As shown in Table 1, the face contact ratio ε_β = 0.9415 at β_{ij} = 15° is closer to an integer than ε_β = 1.2442 at β_{ij} = 20°.

Therefore, the fluctuation of TVMS at β_{ij} = 15° is smaller than that at β_{ij} = 20°. For the gear pair 2, the fluctuation of TVMS always decreases with the increasing helix angle (see Fig. 4(b)). This is because that the face contact ratio always increases with the increasing helix angle, as shown in Table 1.

Table 1. Transverse and face contact ratios of gear pairs 1 and 2.

Gear pair 1			Gear pair 2		
Helix angle β_{ij} (°)	Transverse contact ratio ε_t	Face contact ratio ε_β	Helix angle β_{ij} (°)	Transverse contact ratio ε_t	Face contact ratio ε_β
0	1.7865	0	0	1.7024	0
5	1.7763	0.3171	5	1.6932	0.2219
10	1.7459	0.6317	10	1.6658	0.4422
15	1.6957	**0.9415**	15	1.6205	0.6591
20	1.6268	1.2442	20	1.5580	0.8709

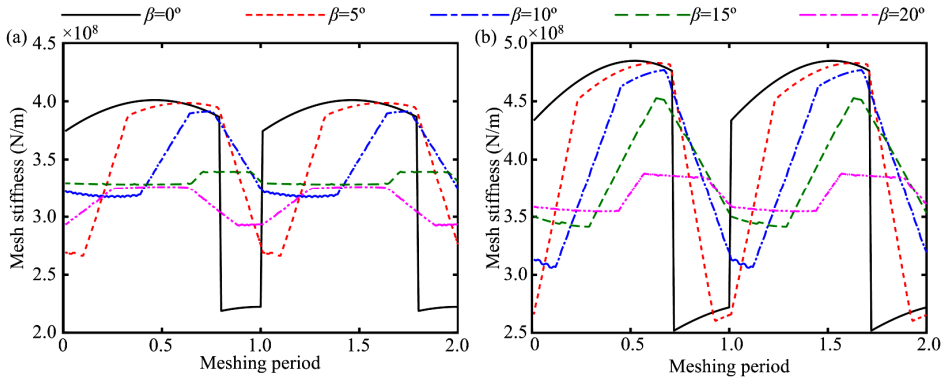

Fig. 4. Mesh stiffness under different helix angles: (a) Gear pair 1; (b) gear pair 2.

3. Dynamic models of geared rotor systems

3.1 Proposed FE model of geared rotor systems

A three-dimensional (3D) mathematical model of a geared rotor system is established (see Fig. 5), which was presented in our earlier paper [9]. Here, we focus on the effects of different coupling models of a gear pair *ij* on vibration characteristics under TVMS excitation. In this section, a lateral and torsional coupling and a lateral, torsional, axial and swing coupling dynamic model of a helical gear pair are developed to study the effects of the gear coupling models, respectively.

A 3D model of a helical gear pair with 12 Degrees of freedom (DOFs) is presented in Fig. 5(b). The displacement vector of a helical gear pair *ij* can be written as follows:

$$\boldsymbol{X}_{ij} = [x_i, y_i, z_i, \theta_{xi}, \theta_{yi}, \theta_{zi}, x_j, y_j, z_j, \theta_{xj}, \theta_{yj}, \theta_{zj}]^{\mathrm{T}}, \tag{12}$$

where x and y are the lateral DOFs, z represents axial DOF, θ_x and θ_y denote swing DOFs and θ_z is the torsional DOF. Considering lateral, torsional, axial and swing coupling, the equations of motion of a helical gear pair *ij* can be written as follows:

$$\boldsymbol{M}_{ij}\ddot{\boldsymbol{X}}_{ij} + (\boldsymbol{C}_{ij} + \boldsymbol{G}_{ij})\dot{\boldsymbol{X}}_{ij} + \boldsymbol{K}_{ij}\boldsymbol{X}_{ij} = \boldsymbol{F}_{ij}, \tag{13}$$

where $\boldsymbol{M}_{ij}$, $\boldsymbol{C}_{ij}$, $\boldsymbol{G}_{ij}$ and $\boldsymbol{K}_{ij}$ denote the mass matrix, damping matrix, gyroscopic matrix and mesh stiffness matrix of the gear pair *ij*. $\boldsymbol{F}_{ij}$ is the excitation force vector, and only a constant torque in applied in this paper. All of those matrices can be found in Ref. [9].

The mesh stiffness matrix $\boldsymbol{K}_{ij}$ (see Fig. 6) can be written as follow:

$$\boldsymbol{K}_{ij} = k_{ij}\boldsymbol{\alpha}_{ij}^{\mathrm{T}} \cdot \boldsymbol{\alpha}_{ij}, \tag{14}$$

where k_{ij} is the mesh stiffness of the helical gear pair, $\boldsymbol{\alpha}_{ij}$ can be expressed as follow:

$$\begin{aligned}\boldsymbol{\alpha}_{ij} = [&-\sin\psi_{ij}\cos\beta_{ij}, \cos\psi_{ij}\cos\beta_{ij}, \mathrm{sgn}\times\sin\beta_{ij},\\ &r_{bi}\sin\psi_{ij}\sin\beta_{ij}, -r_{bi}\cos\psi_{ij}\sin\beta_{ij}, \mathrm{sgn}\times r_{bi}\cos\beta_{ij},\\ &\sin\psi_{ij}\cos\beta_{ij}, -\cos\psi_{ij}\cos\beta_{ij}, -\mathrm{sgn}\times\sin\beta_{ij},\\ &r_{bj}\sin\psi_{ij}\sin\beta_{ij}, -r_{bj}\cos\psi_{ij}\sin\beta_{ij}, \mathrm{sgn}\times r_{bj}\cos\beta_{ij}]\end{aligned} \tag{15}$$

where ψ_{ij}, β_{ij}, sgn denote the angle between the plane of action and positive y-axis direction, helix angle, sign function of the rotation direction of the gear i, respectively. The detailed information for these parameters can be found in Ref. [9].

The upper-left matrix elements in $\boldsymbol{K}_{ij}$ denote the driving gear DOFs, and the lower-right matrix elements denote the driven gear DOFs (see Fig. 6). The upper-right and lower-left matrix elements denote the couple DOFs of the driving and the driven gears. The 144 elements in $\boldsymbol{K}_{ij}$ (see Fig. 6) are all nonzero, which denotes the lateral-torsional-axial-swing coupling. In this paper, the lateral-torsional-axial-swing coupling is also called full coupling. Only the elements in red boxes are nonzero and other elements are all zero, which denotes the lateral-torsional coupling. Considering the lateral-torsional coupling effect, $\boldsymbol{\alpha}_{ij}$ can be rewritten as follows:

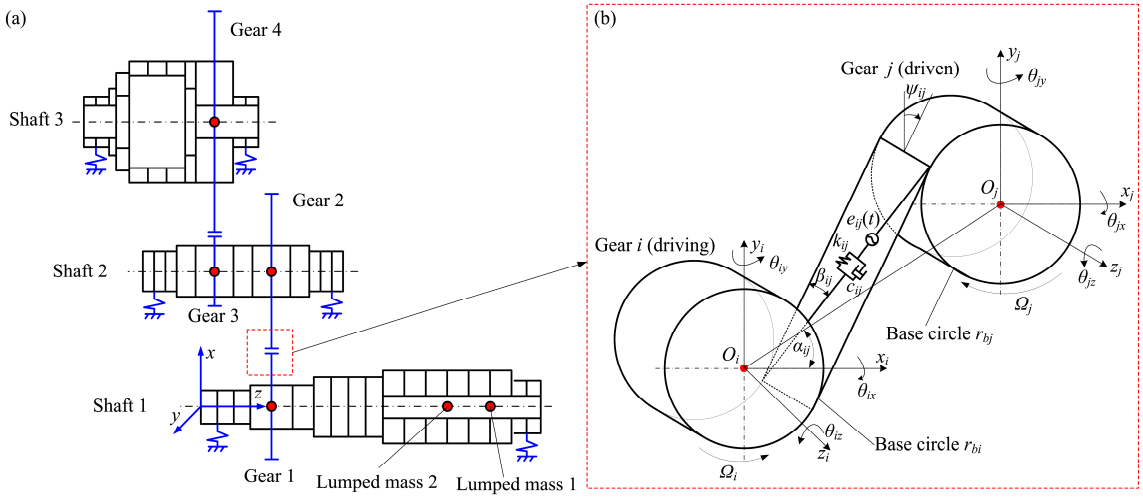

Fig. 5. (a) Schematic of a helical gear rotor system; (b) 3D model of a helical gear pair.

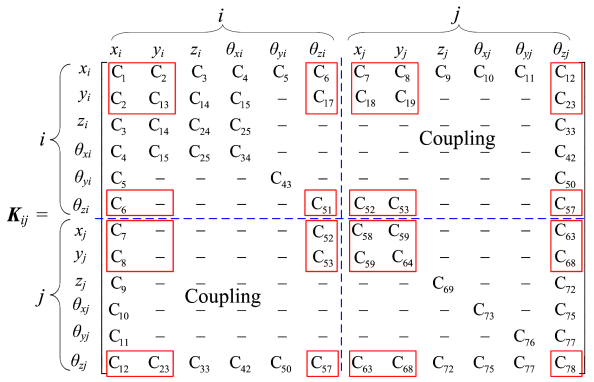

Fig. 6. Mesh stiffness form of the gear pair.

$$\begin{aligned}\boldsymbol{\alpha}_{ij} = [&-\sin\psi_{ij}\cos\beta_{ij}, \cos\psi_{ij}\cos\beta_{ij}, 0, 0, 0,\\ &\mathrm{sgn}\times r_{bi}\cos\beta_{ij}, \sin\psi_{ij}\cos\beta_{ij}, -\cos\psi_{ij}\cos\beta_{ij},\\ &0, 0, 0, \mathrm{sgn}\times r_{bj}\cos\beta_{ij}]\,.\end{aligned} \tag{16}$$

Combining the lumped mass models of gear pairs with the FE models of the shafts, equations of motion of the entire system can be written as:

$$\boldsymbol{M}\ddot{\boldsymbol{u}} + (\boldsymbol{C} + \boldsymbol{G})\dot{\boldsymbol{u}} + \boldsymbol{K}\boldsymbol{u} = \boldsymbol{F}_u\,, \tag{17}$$

where $\boldsymbol{M}$, $\boldsymbol{C}$, $\boldsymbol{K}$, $\boldsymbol{G}$ and $\boldsymbol{F}_u$ are the mass matrix, damping matrix, stiffness matrix, gyroscopic matrix and external force vector of the system, respectively. The Rayleigh-type damping is adopted, and detailed description of these matrices can be found in Ref. [9].

3.2 Identification of dominant mode and shaft based on strain energy

In a gear rotor system, many modal components of different shafts in different directions are coupled in the process of the system vibration calculation. To distinguish the dominant mode and the dominant shaft which has a maximum deformation, the strain energy is adopted, and the strain energy of the ith order of the shafts can be written as follows [18]:

$$\boldsymbol{E}_j^i = \frac{1}{2}\boldsymbol{x}_j^{i\mathrm{T}}\boldsymbol{k}_j\boldsymbol{x}_j^i\,, \tag{18}$$

where $\boldsymbol{x}_j^i$, $\boldsymbol{k}_j$ denote displacement vector and stiffness matrix of the shaft j, respectively. Note that the gears are included into the shafts. Modal strain energy of the system is the sum of modal strain energy of the different shafts. In the analysis of natural characteristics, the bigger ratio of strain energy of each shaft to the strain energy of the system is the dominant shaft. It reflects the shaft has the greatest deformation energy in this order mode. The strain energy ratio v_j^i of shaft j in ith order can be expressed as follows:

$$v_j^i = \frac{\boldsymbol{E}_j^i}{\boldsymbol{E}_{\mathrm{sys}}^i}\,, \tag{19}$$

where $\boldsymbol{E}_{\mathrm{sys}}^i$ denotes the train energy of the ith order of the system. Similarly, the dominant mode can be determined according to the strain energy. The mode of system and shaft can be described as lateral, torsional, axial and swing motions.

An FE model in ANSYS software is established to verify the identification method using strain energy, as shown in Fig. 7. The shafts, gears, bearing are simulated as Beam 188, Mass 21, Matrix 27 elements, respectively. The meshing of the helical gear pair is simulated using Matrix 27 element. The real constants of this Marix 27 element are determined by the elements of the gear mesh stiffness matrix.

Flow chart of the simulation including the TVMS calculation and dynamic characteristics analysis under two coupling models is shown in Fig. 8. The whole analytical procedure can be divided into two parts. First, the TVMS of a helical gear

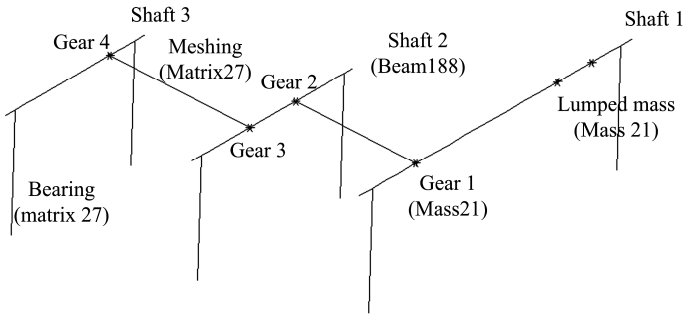

Fig. 7. FE model of the geared rotor system.

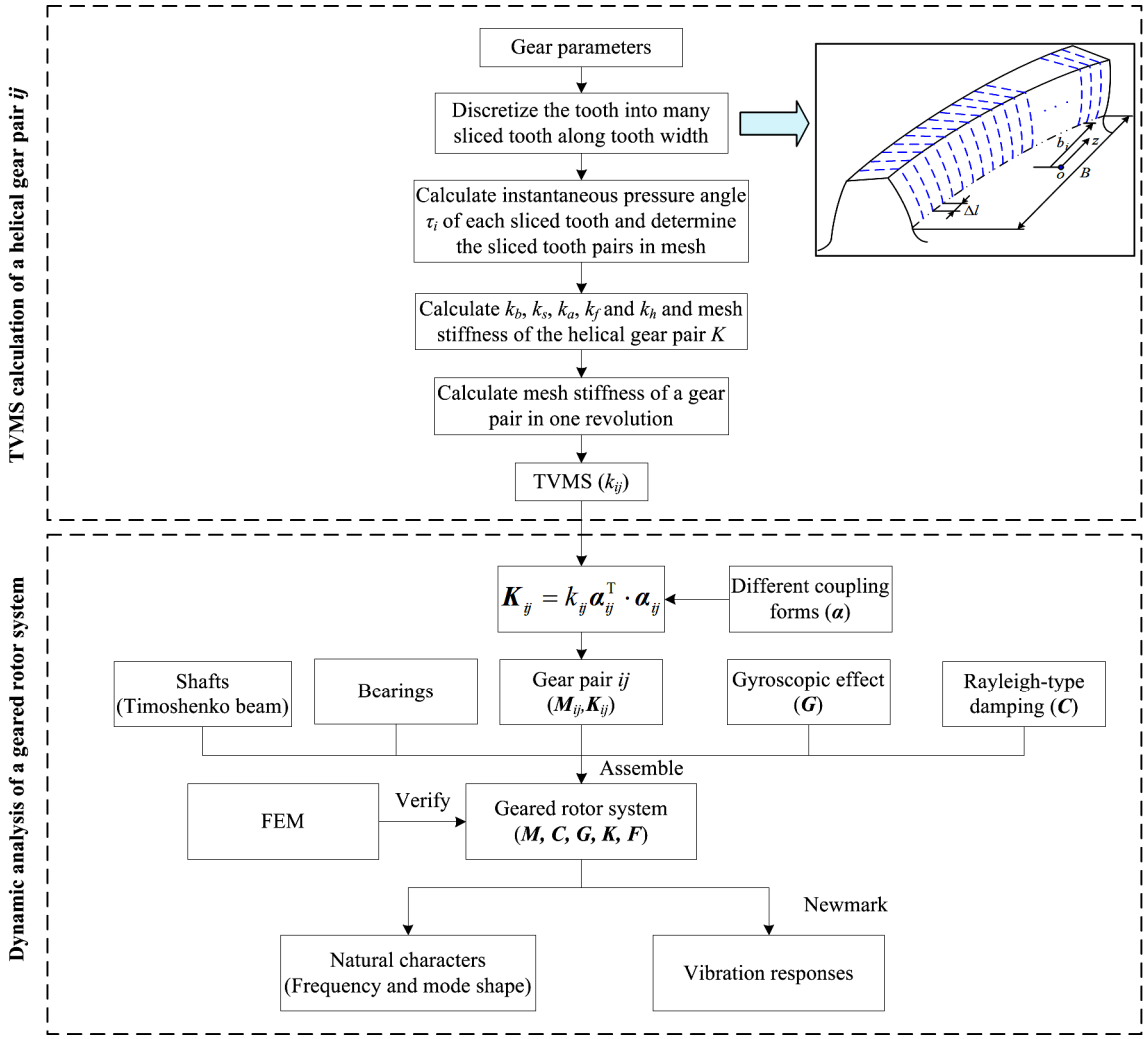

Fig. 8. Flow chart of the simulation.

pair is calculated by the sliced tooth theory based on our earlier work in Ref. [2]. Second, to investigate the influence of different coupling models, a geared rotor system is established, in which the gear pair model is simulated by a lumped mass model, considering the TVMS and constant load torque. The meshing stiffness matrix $\boldsymbol{K}_{ij}$ will change according to the different coupling models.

4. Validation of the dynamic model

As shown in Fig. 9, the experimental equipment coming from Ref. [8] is used for validation of the dynamic model. The helical gear system is shown in Fig. 9(b) and the main design parameters of the helical gear system are listed in Table 2. Some parameters of the helical gear system are not provided

Table 2. Design parameters of the helical gear system in Ref. [8].

Shaft parameters (mm)					
	d_1	d_2	l_1	l_2	l_3
All	37.6	43	100	100	50

Gear parameters		
Parameters	Pinion	Gear
Teeth number	50	50
Transverse module (mm)	3	
Transverse pressure angle (°)	20	
Helix angle (°)	25.232	
Face width (mm)	20	
Applied torque (N·m)	150	

Bearing parameters			
All	k_{xx} (N/m)	k_{yy} (N/m)	k_{zz} (N/m)
	1.7×10^8	1.7×10^8	7.6×10^7
	$k_{\theta x\theta x}$ (N·m/rad)	$k_{\theta y\theta y}$ (N·m/rad)	$k_{\theta z\theta z}$ (N·m/rad)
	1×10^6	1×10^6	0

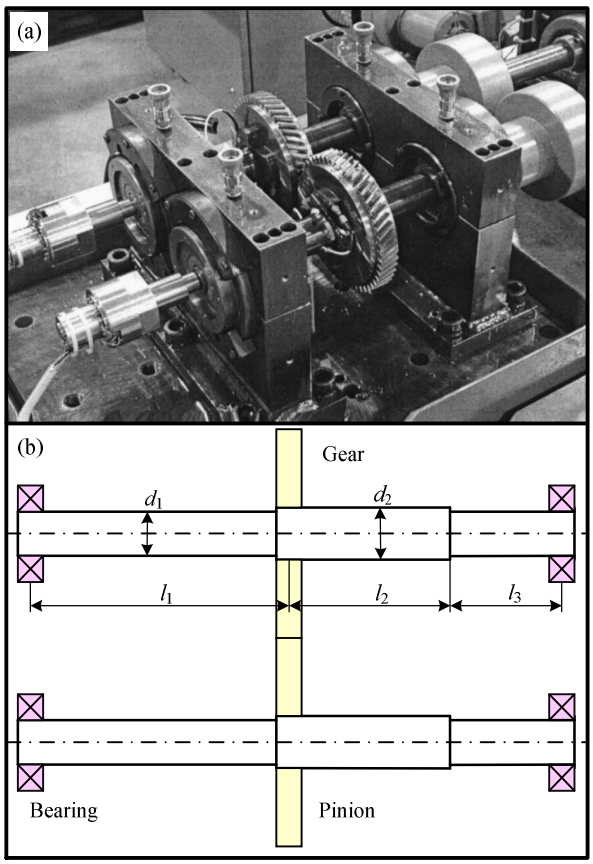

Fig. 9. (a) Test rig; (b) schematic of a gear rotor system in Ref. [8].

in Ref. [8], and here we assume the values of these parameters. The dynamic transmission errors of the helical gear system obtained by the experiment and the proposed model are shown in Fig. 10. As it can be seen, the measured value of DTE basically agrees well with the predicted values of DTE. In the low

Table 3. Parameters of gears.

Gear	$I_x = I_y$ (kg.mm^2)	I_z (kg.mm^2)	m (kg)	Pitch diameter	Hand
1	830	**1660**	0.95	91.0	Left
2	2200	4400	1.22	126.0	Right
3	30	60	0.29	55	Left
4	1500	30000	4.67	197.5	Right

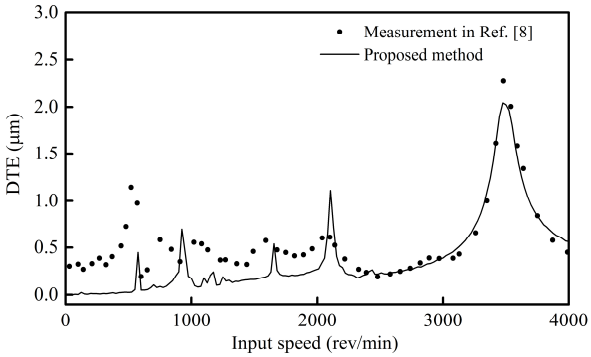

Fig. 10. Comparison of the measured and predicted DTE amplitudes of the helical gear pair by the proposed method.

speed region (0-1000 rev/min), there is a small difference between the measured value and predicted value. This is because the bearing stiffness is unknown and is assumed in this study. This also suggests that the proposed model of a gear rotor system is effective to calculate the vibration responses.

5. Dynamic characteristics comparison using two coupling models

In this section, adopting two coupling models, the natural characteristics and the identification of dominant mode and shaft are analyzed in Sec. 5.1, and the vibration responses are evaluated in Sec. 5.2. The adopted FE model is shown in Fig. 5, the gear parameters can be found in Sec. 2 and Table 3, and the detailed shaft and bearing parameters can be found in Refs. [8, 9].

5.1 Comparison of the natural characteristics using two different coupling models

Generally, the mesh stiffness of the helical gear pairs is time-variable periodically (see Fig. 4). To calculate natural frequencies of the helical geared rotor system, the averaging mesh stiffness needs to be adopted. Based on the TVMS at β_{ij} = 20° in Fig. 4, the averaged mesh stiffness of the gear pair 1 is calculated as 3.13×10^8 N/m and that of gear pair 2 is calculated as 3.69×10^8 N/m.

Natural frequencies and strain energy of each shaft are analyzed by the proposed model and FE model in ANSYS software, as listed in Tables 4 and 5. For the geared rotor system and shaft 2, the dominant mode of each order natural frequency is also analyzed, as shown in Tables 6 and 7, respectively. These tables show the following phenomena:

Table 4. Natural frequencies and strain energy by the proposed model.

No.	Full coupling					Lateral-torsional coupling				
	Natural frequencies	Dominant shaft	Strain energy (%)			Natural frequencies	Dominant shaft	Strain energy (%)		
			Shaft 1	Shaft 2	Shaft 3			Shaft 1	Shaft 2	Shaft 3
1	817.3	2	33.9	55.2	10.9	845.9	2	36.3	55.0	8.7
2	1343.9	1	80.2	12.3	7.5	1358.4	1	81.0	13.1	5.9
3	**1453.3**	**1**	**100**	**0**	**0**	**1453.3**	**1**	**100**	**0**	**0**
4	1671.8	1	90.4	5.2	4.4	1675.5	1	90.2	5.9	3.9
5	**2322.0**	**3**	**0**	**0**	**100**	**2322.0**	**3**	**0**	**0**	**100**
6	2345.2	3	2.1	4.5	93.4	2352.5	3	0	0	100
7	2364.3	3	8.9	18.3	72.8	2361.1	3	8.0	21.3	70.7
8	2543.3	2	15.9	74.5	9.6	2532.3	2	11.7	81.5	6.8
9	2657.1	1	91.1	8.7	0.2	2662.5	1	100	0	0
10	2844.8	2	21.6	43.5	34.9	2934.9	2	38.4	46.3	15.4

Table 5. Natural frequencies and strain energy by FE model in ANSYS software.

No.	Full coupling					Lateral-torsional coupling				
	Natural frequencies	Dominant shaft	Strain energy (%)			Natural frequencies	Dominant shaft	Strain energy (%)		
			Shaft 1	Shaft 2	Shaft 3			Shaft 1	Shaft 2	Shaft 3
1	818.7	2	38.5	55.1	6.4	847.3	2	40.3	54.7	5.0
2	1352.0	1	81.5	14.0	4.5	1367.0	1	81.5	14.9	3.6
3	**1468.0**	**1**	**100**	**0**	**0**	**1468.0**	**1**	**100**	**0**	**0**
4	1679.1	1	93.3	.4.6	2.1	1682.4	1	93.0	5.2	1.8
5	**2334.5**	**3**	**0**	**0**	**100**	**2334.5**	**3**	**0**	**0**	**100**
6	2349.4	3	2.7	4.2	93.1	2352.5	3	0	0	100
7	2369.7	3	21.3	32.6	46.1	2370.4	3	14.5	27.9	57.6
8	2547.9	2	16.1	77.7	6.2	2537.2	2	14.8	81.0	4.2
9	2657.5	1	69.8	29.8	0.4	2662.5	1	100	0	0
10	2834.2	2	14.1	45.3	40.6	2928.1	2	18.3	41.8	39.9

Table 6. Modal strain energy of geared rotor systems.

No.	Full coupling						Lateral-torsional coupling					
	Natural frequencies	Dominant mode	Modal strain energy (%)				Natural frequencies	Dominant mode	Modal strain energy (%)			
			Lateral	Torsional	Axis	Swing			Bending	Torsion	Axial	Swing
1	817.3	Torsional	5.7	93.5	0.2	0.6	845.9	Torsional	6.4	93.1	0	0.5
2	1343.9	Lateral	51.0	44.6	0.2	4.3	1358.4	Torsional	54.0	41.7	0	4.3
3	**1453.3**	Lateral	**92.5**	**0**	**0**	**7.5**	**1453.3**	Lateral	**92.5**	**0**	**0**	**7.5**
4	1671.8	Torsional	37.7	58.9	0.3	3.1	1675.5	Torsional	35.2	61.8	0	3.0
5	**2322.0**	Lateral	**91.9**	**0**	**0**	**8.1**	**2322.0**	Lateral	**91.9**	**0**	**0**	**8.1**
6	2345.2	Axial	42.1	2.6	51.5	3.8	2352.5	Axial	0	0	100	0
7	2364.3	Axial	40.3	10.8	44.9	4.0	2361.1	Lateral	82.1	10.1	0	7.8
8	2543.3	Lateral	71.8	15.8	5.6	6.8	2532.3	Lateral	75.0	16.7	0	8.3
9	2657.1	Axial	8.1	0.5	90.2	1.2	2662.5	Axial	0	0	100	0
10	2844.8	Lateral	54.0	17.5	4.7	23.8	2934.9	Lateral	63.1	23.3	0	13.6

(1) From Tables 4 and 5, the natural frequencies and the dominant shaft obtained from the proposed model agree well with that obtained from FE model in ANSYS software. The maximum relative error of natural frequency is less than 1 %.

(2) There is a slight difference of natural characteristics between full coupling and lateral-torsional coupling (see Table 4). For example, the sixth strain energy of shaft 3 is 100 % and strain energy of shafts 1 and 2 is zero for lateral-torsional

Table 7. Modal strain energy of shaft 2.

No.	Full coupling						Lateral-torsional coupling					
	Natural frequencies	Dominant mode	Modal strain energy (%)				Natural frequencies	Dominant mode	Modal strain energy (%)			
			Lateral	Torsional	Axial	Swing			Lateral	Torsional	Axial	Swing
1	817.3	Lateral	64.5	26.9	3.7	4.9	845.9	Lateral	69.9	29.5	0	0.6
2	1343.9	Lateral	52.0	44.2	1.5	2.3	1358.4	Lateral	55.2	43.0	0	1.8
3	**1453.3**	No-vibration	**0**	**0**	**0**	**0**	**1453.3**	No-vibration	**0**	**0**	**0**	**0**
4	1671.8	Lateral	62.9	30.2	0.6	6.3	1675.5	Lateral	67.7	30.3	0	2.0
5	**2322.0**	No-vibration	**0**	**0**	**0**	**0**	**2322.0**	No-vibration	**0**	**0**	**0**	**0**
6	2345.2	Lateral	88.4	1.2	0.6	9.8	2352.5	No-vibration	0	0	0	0
7	2364.3	Lateral	89.0	0.7	0.5	9.8	2361.1	Lateral	91.0	1.3	0	7.7
8	2543.3	Lateral	92.2	0.8	0	7.0	2532.3	Lateral	90.1	0.7	0	9.2
9	2657.1	Lateral	86.3	0.3	0	13.4	2662.5	No-vibration	0	0	0	0
10	2844.8	Lateral	71.4	10.4	0.5	17.7	2934.9	Lateral	76.2	15.1	0	8.7

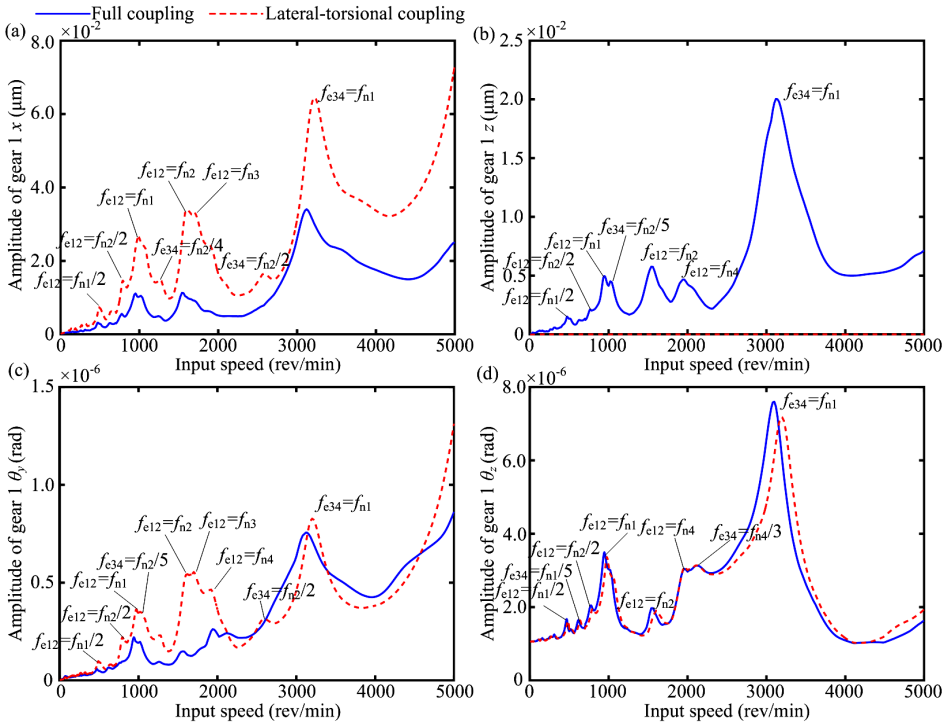

Fig. 11. Vibration responses of the gear 1: (a) x-direction; (b) z-direction; (c) θ_y-direction; (d) θ_z-direction.

coupling; however, all the shafts have the strain energy for full coupling (see Table 4). Besides, the sixth modal strain energy in axial direction is 100 % for lateral-torsional coupling and that is 51.5 % for full coupling (see Table 6). These results revealed that axial and swing motions cannot be ignored for accurately determining the system natural characteristic.

(3) Under full coupling and lateral-torsional coupling, the third strain energy of shaft 1 is 100 % and strain energy of shafts 2 and 3 is zero (see Table 4). It reveals that there is a weak coupling due to gear meshing among the shafts under some cases.

(4) Taking the third-order mode as an example, the strain energy of shaft 1 is 100 % (see Table 4) and the dominant modal strain energy of the system is lateral-swing motion (see Table 6). Only the shaft 1 shows the lateral vibration in this order by observing the corresponding modal shape (shown in Ref. [9]). Besides the identification of geared rotor systems, the modal strain energy of one single shaft (shaft 2) can be also identified, as shown in Table 7. From above analysis, the strain energy can be used to distinguish the dominant mode shape and dominant shaft.

5.2 Comparison of the vibration responses using two different coupling models

Based on the FE model of the helical geared rotor system

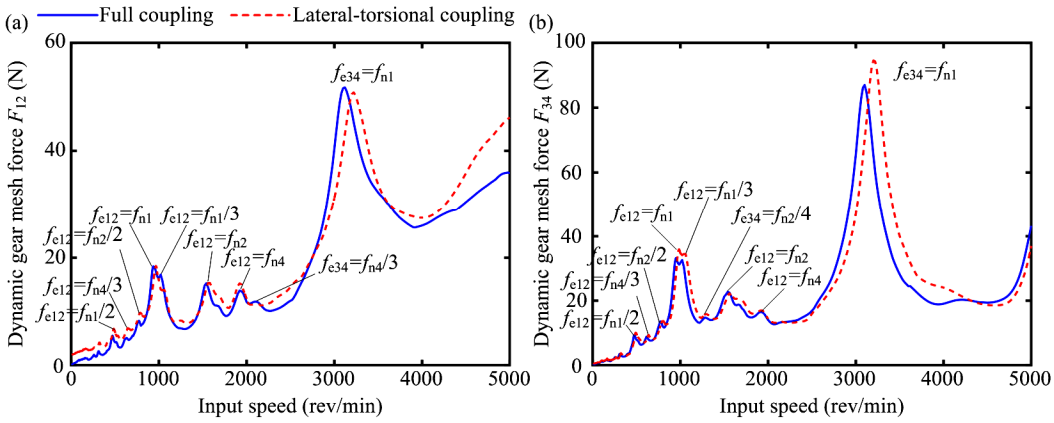

Fig. 12. Dynamic mesh forces: (a) Gear pair 1; (b) gear pair 2.

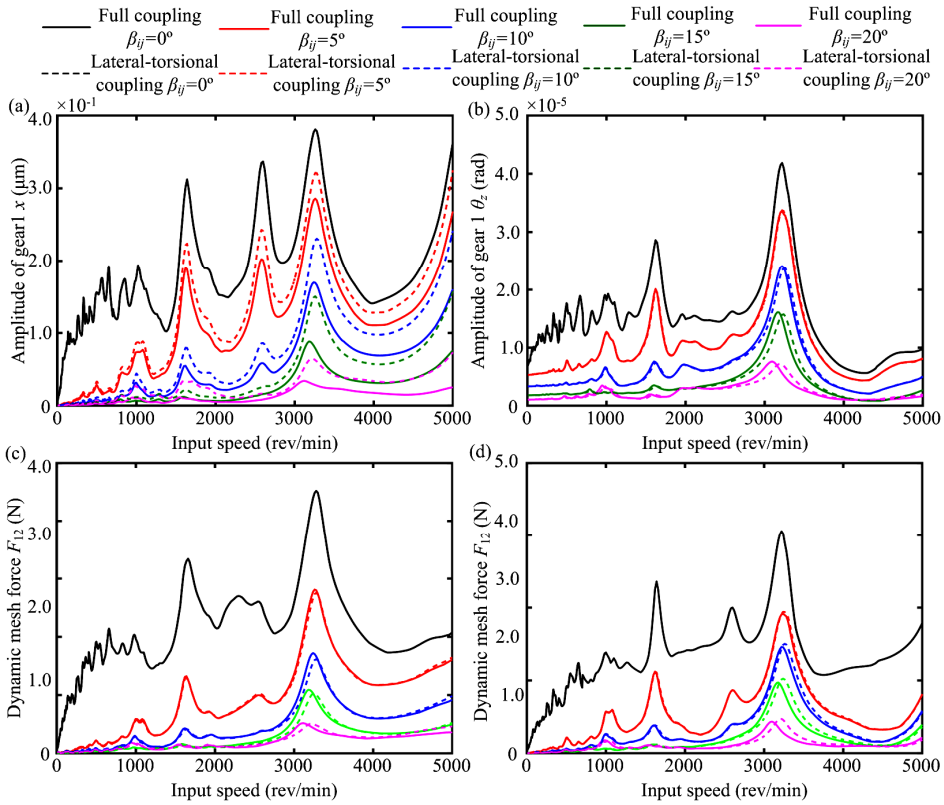

Fig. 13. Vibration responses of gear 1 and dynamic mesh forces of gear pairs 1 and 2: (a) x-direction; (b) θ_z-direction; (c) dynamic mesh force of gear pair 1; (d) dynamic mesh force of gear pair 2.

developed in Sec. 3, vibration responses of the gear system are studied under the TVMS excitation using two different coupling models. The applied load torque is 50 Nm. Vibration responses of the gear 1 and dynamic mesh forces of the gear pairs 1 and 2 are shown in Figs. 11 and 12, respectively.

The responses in θ_z direction using two coupling models are very close and those in x, z, θ_y directions have a bigger error. This is because axial (z direction) and swing (θ_x and θ_y directions) vibration cannot be considered in the lateral-torsional coupling model. Therefore, the full coupling model could predict accurately the responses of a helical gear system. However, the lateral-torsional coupling model can cause some errors for predicting the responses of the helical gear system. Both the two models can predict effectively the dynamic mesh force of the gear pair (see Fig. 12). There are some resonance peaks of gear 1 in Fig. 11. These resonance frequencies occur when the gear mesh frequencies f_{e12} and f_{e34} are equal to $f_{n1}/2$, $f_{n2}/4$, $f_{n2}/2$, f_{n1}, f_{n2}, f_{n3} and f_{n4}, respectively. It reveals that the super-harmonic resonances may occur because of the TVMS excitation in two coupling models.

The vibration responses of gear 1 and the dynamic mesh forces under different helix angles are shown in Fig. 13, which

shows the following vibration characteristics of geared rotor systems.

(1) The amplitudes of vibration responses and the dynamic mesh forces decrease with the increasing helix angles, which is related to the TVMS fluctuation.

Note that the fluctuation of TVMS of gear pair 1 under β_{ij} = 20° is larger than that under β_{ij} = 15° (see Fig. 4); however, under most rotational speeds, the vibration response of gear pair 1 at β_{ij} = 20° is smaller than that of gear pair 1 at β_{ij} = 15°.

(2) The vibration responses obtained from two coupling models are the same at β_{ij} = 0°, namely, the axial and swing coupling vibrations have no effects on the spur gear. The axial and swing coupling effects increase with the increasing helix angles. The shifting of the resonant peaks due to different coupling levels can clearly observed at β_{ij} = 15° and β_{ij} = 20° (see Figs. 13(a) and (b)).

6. Conclusions

In this study, we analyzed the combined effects of Time-varying mesh stiffness (TVMS) and gear coupling level on the dynamic characteristics of a helical geared rotor system. Two types of coupling, lateral-torsional-axial-swing coupling (also known as full coupling in this paper) and lateral-torsional coupling, are compared by natural frequencies, modal strain energy and vibration responses. dynamic characteristics of a helical geared rotor system are analyzed. Some conclusions are summarized as follows:

(1) The modal strain energy can be used to distinguish the dominant mode and shaft of geared rotor systems, which can contribute to identify the coupling level of the system.

(2) The responses of a helical gear system in torsional direction and dynamic mesh force obtained from two coupling models are almost the same. However, there exist larger differences in the lateral and axial vibrations. This also suggests that the axial and swing coupling cannot be ignored to accurately predict the vibration response of the system. Due to the TVMS excitation, super-harmonic resonances can be observed in the amplitude-frequency responses.

(3) The fluctuation value of TVMS decreases when the face contact ratio is close to an integer; for example, the TVMS fluctuation at helix angle β_{ij} = 15° is smaller than that at β_{ij} = 20°. The amplitudes of vibration responses and the dynamic mesh forces decrease with the increasing helix angles, which is related to the TVMS fluctuation. It is worth noting that the vibration response of gear pair 1 at β_{ij} = 20° is smaller than that of gear pair 1 at β_{ij} = 15°, which is due to the combined effects of gear pair coupling and the fluctuation of TVMS.

Acknowledgment

This project is supported by the Joint Funds of the National Natural Science Foundation and the Civil Aviation Administration of China (Grant No. U1433109), the National Natural Science Foundation of China (Grant No. 51605361), the Fundamental Research Funds for the Central Universities (Grant Nos. N150305001, XJS16041 and JB160411), and State Key Laboratory for Strength and Vibration of Mechanical Structures (Grant No. SV2015-KF-08) and are thanked for providing financial support for this work.

Nomenclature

$\boldsymbol{E}_j^i$, $\boldsymbol{x}_j^i$, $\boldsymbol{k}_j$: Strain energy of the ith order, stiffness matrix and displacement vector of the shaft j

$\boldsymbol{E}_{\text{sys}}^i$: Strain energy of the ith order of the system

$\boldsymbol{F}_{ij}$: Excitation force vector

$\boldsymbol{M}_{ij}$, $\boldsymbol{C}_{ij}$, $\boldsymbol{G}_{ij}$ and $\boldsymbol{K}_{ij}$: Mass matrix, damping matrix, gyroscopic matrix and mesh stiffness matrix of the gear pair ij

$\boldsymbol{M}$, $\boldsymbol{C}$, $\boldsymbol{K}$, $\boldsymbol{G}$ and $\boldsymbol{F}_u$: Mass matrix, damping matrix, stiffness matrix, gyroscopic matrix and external force vector of the system

k_h, k_b, k_s, k_a and k_f : Hertzian contact stiffness, bending stiffness, shear stiffness, axial compressive stiffness and gear foundation stiffness

k_i, k_j : Mesh stiffness of the sliced tooth pairs i and j

k_{ij} : Mesh stiffness of gear pair

N : Number of sliced tooth pairs in mesh simultaneously

sgn : Sign function

z_1, z_2 : Numbers of the teeth of the pinion and gear

Greek symbols

β_{ij} : Helix angle of base circle

τ_b, τ_e : The minimum and maximum pressure angles

Δl : Width of the sliced tooth pair

ε_t, ε_β : Transverse contact ratio and face contact ratio

ψ_{ij} : The angle between the plane of action and positive y-axis

v_j^i : Strain energy ratio of shaft j

References

[1] Z. Wan et al., Mesh stiffness calculation using an accumulated integral potential energy method and dynamic analysis of helical gears, *Mechanism and Machine Theory*, 92 (2015) 447-463.

[2] Q. Wang and Y. Zhang, A model for analyzing stiffness and stress in a helical gear pair with tooth profile errors, *J. of Vibration and Control*, 23 (2) (2017) 272-289.

[3] X. Gu et al., Analytical investigations on the mesh stiffness function of solid spur and helical gears, *J. of Mechanical Design*, 137 (2015) 063301.1-7.

[4] J. Hedlund and A. Lehtovaara, A parameterized numerical model for the evaluation of gear mesh stiffness variation of a helical gear pair, *Proceedings of the Institution of Mechanical Engineers, Part C: J. of Mechanical Engineering Science,* 222 (2008) 1321-1327.

[5] A. Kahraman, Effect of axial vibraton on the dynamics of a helical gear pair, *J. of Vibration and Acoustics*, 115 (1993)

33-39.
[6] S. H. Choi et al., Dynamic gear loads due to coupled lateral, torsional and axial vibrations in a helical geared system, *J. of Vibration and Acoustics*, 141 (1999) 141-148.
[7] M. Kubur et al., Dynamic analysis of multi-mesh helical gear sets by finite elements, *ASME 2003 International Design Engineering Technical Conferences and Computers and Information in Engineering Conference*, American Society of Mechanical Engineers, September 2-6 (2003).
[8] M. Kubur et al., Dynamic analysis of a multi-shaft helical gear transmission by finite elements: Model and experiment, *J. of Vibration and Acoustics,* 126 (2004) 398-406.
[9] Y. M. Zhang et al., Dynamic analysis of three-dimensional helical geared rotor system with geometric eccentricity, *J. of Mechanical Science and Technology*, 27 (2013) 3231-3242.
[10] M. Kang and A. Kahraman, An experimental and theoretical study of the dynamic behavior of double-helical gear sets, *J. of Sound and Vibration*, 350 (2015) 11-29.
[11] M. R. Kang and A. Kahraman, Measurement of vibratory motions of gears supported by compliant shafts, *Mechanical Systems and Signal Processing*, 29 (2012) 391-403.
[12] P. Velex, J. Bruyère and D. R. Houser, Some analytical results on transmission errors in narrow-faced spur and helical gears: influence of profile modifications, *J. of Mechanical Design*, 133 (2011) 031010.1-10.
[13] T. Nishino, Vibration analysis of the helical gear system using the integrated excitation model, *J. of Advanced Mechanical Design, Systems, and Manufacturing*, 1 (2007) 541-552.
[14] T. Eritenel and R. G. Parker, Three-dimensional nonlinear vibration of gear pairs, *J. of Sound and Vibration*, 331 (2012) 3628-3648.
[15] S. Chen et al., Rotordynamics analysis of a double-helical gear transmission system, *Meccanica,* 51 (2016) 251-268.
[16] M. S. Abbes et al., Effect of transmission error on the dynamic behaviour of gearbox housing, *International J. of Advanced Manufacturing Technology,* 34 (2007) 211-218.
[17] Y. Wu, J. Wang and Q. Han, Static/dynamic contact FEA and experimental study for tooth profile modification of helical gears, *J. of Mechanical Science and Technology,* 26 (2012) 1409-1417.
[18] S. H. Song, M. P. Castanier and C. Pierre, System identification of multistage turbine engine rotors, *ASME Turbo Expo 2007: Power for Land, Sea, and Air*, American Society of Mechanical Engineers (2007) 569-582.
[19] H. Ma et al., Effects of tooth crack on vibration responses of a profile shifted gear rotor system, *J. of Mechanical Science and Technology*, 29 (10) (2015) 4093-4104.
[20] H. Ma et al., Review on dynamics of cracked gear systems, *Engineering Failure Analysis*, 55 (2015) 224-245.

Qibin Wang is a Lecturer at School of Electro-Mechanical Engineering, Xidian University, China. His interests are in geared rotor system dynamic, mechanical reliability, and others.

Hui Ma is a Professor at the School of Mechanical Engineering and Automation, Northeastern University, China. His research interests include rotor dynamics and fault diagnosis.